

# Optical and photoemission evidence for a Tomonaga-Luttinger liquid in the Bechgaard salts

V. Vescoli<sup>1</sup>, F. Zwick<sup>2</sup>, W. Henderson<sup>3</sup>, L. Degiorgi<sup>1,a</sup>, M. Gioni<sup>2</sup>, G. Gruner<sup>3</sup>, and L.K. Montgomery<sup>4</sup>

<sup>1</sup> Laboratorium für Festkörperphysik, ETH Zurich, 8093 Zurich, Switzerland

<sup>2</sup> Institut de Physique Appliquée, École Polytechnique Fédérale de Lausanne, 1015 Lausanne, Switzerland

<sup>3</sup> Department of Physics, University of California at Los Angeles, Los Angeles CA 90095-1547, USA

<sup>4</sup> Department of Chemistry, University of Indiana, Bloomington IN 47405, USA

Received 17 May 1999 and Received in final form 13 July 1999

**Abstract.** Combined optical and photoemission experiments on the quasi-one dimensional Bechgaard salts reveal the non-Fermi liquid character of these prototype quasi-one dimensional interacting electron systems. We show that various aspects of the exotic normal state properties along the chains are consistent with the predictions of the Tomonaga-Luttinger liquid theory. We also discuss the effect of interchain coupling on the insulator-metal transition, associated with the electron confinement-deconfinement crossover.

**PACS.** 78.20.-e Optical properties of bulk materials and thin films – 79.60.-i Photoemission and photoelectron spectra – 71.27.+a Strongly correlated electron systems; heavy fermions

## 1 Introduction

The Fermi liquid (FL) theory is extremely general and robust, and has been one of the cornerstones of the theory of interacting electrons in metals for the last half century. The theory is based on the recognition that the low-lying excitations of an interacting electron system are in a one-to-one correspondence with those of the noninteracting gas, only with renormalized energies. FL theory has been thoroughly tested on a variety of materials and is usually valid in higher than one dimension (1D). One possible notable exception is the normal state of the two-dimensional (2D) copper oxide-based high-temperature superconductors (HTSC). Recently, a great deal of interest has been devoted to the possible breakdown of the FL framework in quasi-one dimensional materials.

In a strictly 1D interacting electron system, the FL state is replaced by a state where interactions play a crucial role, and which is generally referred to as a Tomonaga-Luttinger liquid (TLL). The 1D state predicted by the TLL theory [1] is characterized by features such as spin-charge separation and the absence of a sharp edge in the momentum distribution function  $n(k)$  at the Fermi wave vector  $k_F$  (*i.e.*, by the fact that, in the Fermi liquid language, the renormalization factor  $Z \rightarrow 0$  at  $k_F$ ). The non-Fermi liquid nature of the TLL is also manifested by an absence of single-electron-like quasiparticles and by the non-universal decay of the various correlation functions. The first immediate consequence of the absence of the discontinuity at  $k_F$  in the momentum distribution function

is the powerlaw behaviour of the density of states (DOS)  $\rho(\omega) \sim |\omega|^\alpha$  ( $\omega = E_F - E$ ). The exponent in this expression reflects the nature and strength of the interaction. Figure 1a compares the typical DOS near the chemical potential and at  $T = 0$  for a FL and a TLL scenario (with  $\alpha > 1$ ).

The TLL, which describes gapless 1D fermion systems, may be unstable towards the formation of a spin or a charge gap [2,3]. Spin gaps are obtained in microscopic 1D models including electron-phonon coupling, and are relevant to the description of the normal state of superconductors and Peierls (CDW) insulators [2]. The second instability, which concerns the linear chain Bechgaard salts discussed below, is a more typical consequence of electronic correlations. At half filling, and more generally at commensurate values of band filling  $n = p/q$  (with  $p$  and  $q$  integers), the long-range electron-electron interaction together with Umklapp scattering (which arises when the lattice periodicity is also involved) [3] drive the system to a Mott insulator with a correlation gap in the charge excitation spectrum (*i.e.*, in the real part  $\sigma_1(\omega)$  of the optical conductivity (Fig. 1b)). Strictly speaking, 1D systems with one gapped channel, either charge or spin, do not belong to the universality class of the Tomonaga-Luttinger model, but rather to that of the related Luther-Emery (LE) model [2]. Nevertheless, the two models exhibit several common, typically 1D features, like spin-charge separation. Of course, real materials are only quasi-one-dimensional, and the interchain hopping integrals are finite in the two transverse directions. The electronic ground state is therefore determined by

<sup>a</sup> e-mail: degiorgi@solid.phys.ethz.ch

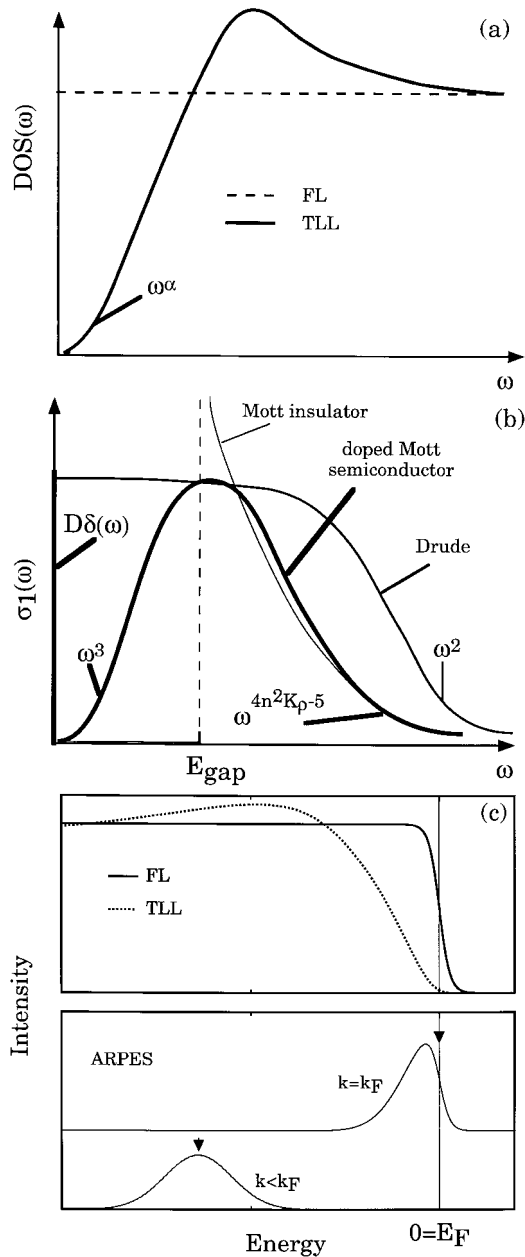


**Fig. 1.** Comparison between the Fermi-liquid and Tomonaga-Luttinger liquid scenarios: (a) density of states, (b) optical conductivity (Mott-insulator, doped Mott semiconductor and Drude behaviour), and (c) Top: FL and TLL spectral functions as obtained in the angle-integrated (PES) experiment; Bottom: angle-resolved (ARPES) spectra illustrating the dispersion and the crossing of the chemical potential (“Fermi surface crossing”) by a quasiparticle peak [3,17].

a competition between the Mott gap (*i.e.*, the 1D limit) and the interchain hopping. In a very crude way, the interchain hopping can be viewed as an effective doping, leading to deviations from the commensurate filling (which is insulating).

The spectral properties of both metallic and gapped 1D systems reflect the unusual nature of correlations in 1D. Therefore, optics and photoemission, especially on

single crystal samples, are powerful tools to address the above fundamental issues. The optical response has been also calculated for a doped one-dimensional Mott semiconductor and consist of a Mott gap (as reminder of the original 1D limit) and a zero-energy mode (representing the effective metallic contribution) for small doping levels (Fig. 1b) [3]. Of course for the low-energy mode, this is an oversimplified view, since the interchain hopping makes the system two-dimensional, and the low-energy feature is unlikely to be described by a simple one-dimensional theory [3]. Such an interchain coupling becomes ineffective at high enough temperatures or frequencies, and thus we would expect the 1D physics (*i.e.*, the Mott insulating state) to dominate in this regime, where a powerlaw behaviour in  $\sigma_1(\omega)$  is expected in both limits (Fig. 1b) [3]. While the high temperature dc conductivity has essentially a metallic character in most linear chain compounds [4], the finite frequency optical response is distinctly non-Drude [5–7].

Non-Fermi liquid features should also be visible in the photoemission spectra. The  $k$ -integrated spectrum of the Luttinger model vanishes at the chemical potential ( $E_F$ ) as a power law. By contrast, a normal metal is characterized by a finite intensity at  $E_F$ , and by a temperature- and resolution-limited edge – the metallic Fermi step – (Fig. 1c). Distinct spectral features, the holon and the spinon, reflecting spin-charge separation, are also expected to replace the dispersing quasiparticle peaks in the  $k$ -resolved (ARPES) spectra [8,9]. Correspondingly in angle-integrated (PES) spectra the intensity near the chemical potential is strongly renormalized (Fig. 1c) [10].

In this paper we show that the combined insights from optics and photoemission support a TLL scenario in the linear-chain organic Bechgaard salts. We also discuss the dimensionality crossover which progressively drives the systems from a 1D Mott insulator to a quasi-2D Fermi liquid metal, under the effect of increasing transverse (*i.e.*, perpendicular to the 1D chains) interactions. Parts of this work, and several technical details have been separately presented elsewhere [7,11,12]. After a short introduction on the Bechgaard salts and a reminder of the experimental techniques, we first illustrate the most relevant results. We discuss them by exploring possible scenarios, alternative to the FL approach. The conclusion summarizes several open issues and gives an outlook on future research.

## 2 Experiment and results

### 2.1 Bechgaard salts

Since their first synthesis in the late 1970 [13], the  $(TMTSF)_2X$  family of linear-chain organic conductors, and the closely related TMTTF family, have attracted continual attention. While the various broken symmetry ground states, including spin-density waves, charge-density waves, spin Peierls, and even superconductivity have been extensively explored over the last two decades [4,14,15], much of the current attention is now

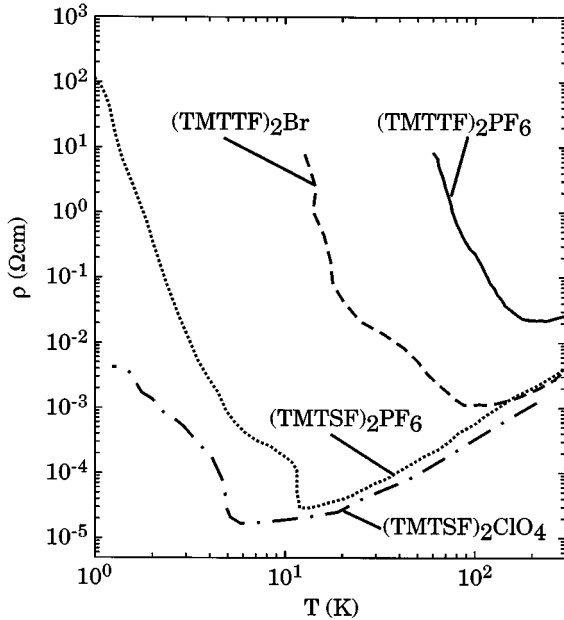


**Fig. 2.** Temperature dependence of the resistivity for  $(\text{TMTTF})_2\text{X}$  and  $(\text{TMTSF})_2\text{X}$  measured along the chain axis. The data are taken on our samples and are in agreement with previously published results [4, 13, 20].

focused on the (metallic) normal state, because of the issues pointed out above [16, 17]. These compounds have become one of the prototypical testing grounds for the study of the effects of electron-electron interactions in one-dimensional structures. In the Bechgaard salts, charge transfer of one electron from every two TMTSF molecules leads to a quarter-filled (or half-filled due to the dimerization of the TMTSF and TMTTF molecules along the chain axis [4]) hole band, thus making Umklapp scattering relevant [18].

Many of the measurements presented here were made possible by our ability to grow large single crystals of the Bechgaard salts. The large single crystals used in this study were grown by the standard electrochemical growth techniques [13], but at reduced temperature (0 °C) and at low current densities. These conditions produce a slow growth rate and, over a period of 4–6 months, single crystals up to  $4 \times 2.5 \times 1 \text{ mm}^3$ . These large, high-quality crystal faces in the  $a$ – $b'$  plane allowed us to perform reliable measurements of the electrodynamic response and photoemission spectra of these materials both parallel ( $E||a$ ) and perpendicular ( $E||b'$ ) to the highly conducting chain axis down to low frequencies [19].

Figure 2 displays the resistivity  $\rho(T)$  of the Bechgaard salt compounds that we have measured along the linear chain axis. There is a good agreement with the literature data [4, 13, 20]. The  $(\text{TMTSF})_2\text{X}$  salts have a clear metallic behaviour down to  $T_{\text{SDW}}$  of 12 and 6 K for  $\text{X} = \text{PF}_6$  and  $\text{ClO}_4$ , respectively, where the SDW phase transition takes place. The TMTTF salts, on the other hand, have a first metal-insulator phase transition at  $T_\rho \sim 100$ – $200$  K. Such an insulating phase was ascribed to charge localization [4, 21]. Below temperatures of about 10 K,

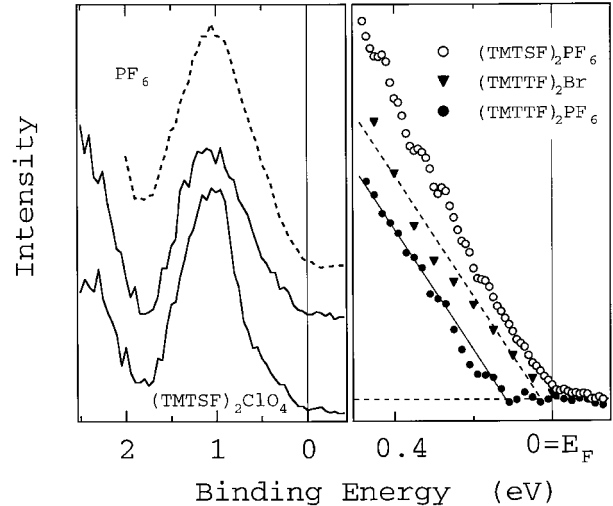


**Fig. 3.** Left: PES spectrum of  $(\text{TMTSF})_2\text{PF}_6$  (dashed line) showing no intensity at  $E_F$ . The solid lines are ARPES spectra of  $(\text{TMTSF})_2\text{ClO}_4$ , measured at the  $\Gamma$  point (bottom) and at the zone boundary (middle), in the chain direction ( $T = 150$  K). Right: Comparison of normal emission ARPES spectra of three Bechgaard salts. The extrapolation of the leading edges of the spectra defines a material-dependent energy gap.

there is a spin-Peierls and a SDW phase transition for  $(\text{TMTTF})_2\text{PF}_6$  and  $(\text{TMTTF})_2\text{Br}$ , respectively [4, 22].

## 2.2 Photoemission

For our photoemission measurements we used both polarized synchrotron radiation (at the Wisconsin Synchrotron Radiation Center), and unpolarized HeI radiation ( $h\nu = 21.2$  eV, at Lausanne). The experimental energy resolution varied between 10 meV and 30 meV, and the momentum resolution was  $\Delta k \sim 0.04 \text{ \AA}^{-1}$  at 21.2 eV. We determined the Fermi level position with an accuracy of  $\pm 5$  meV from the spectra of evaporated Au films.

Figure 3 illustrates representative PES and ARPES spectra of the Bechgaard salts. The angle integrated PES spectrum of  $(\text{TMTSF})_2\text{PF}_6$  exhibits a prominent feature at 1 eV, a binding energy which corresponds to the bottom of the conduction band [23]. Remarkably, the intensity is vanishingly small at the Fermi level, in apparent contradiction with the metallic character of this material (see Fig. 1c). The strong spectral weight renormalization is consistent with photoemission data on other quasi-1D materials [10, 11, 24–29]. The leading edge of the spectrum could be fitted over a broad energy range by a power-law lineshape, with an exponent of order 1.

The unusual lineshape is confirmed by the ARPES spectra of  $(\text{TMTSF})_2\text{ClO}_4$ , in the normal state. Within our experimental accuracy, these data are also indistinguishable from those of  $(\text{TMTSF})_2\text{PF}_6$ . These spectra exhibit a strong polarization dependence: the intensity within 1.5 eV of  $E_F$  is enhanced when the electric field vector is parallel to the chains, as in Figure 3 [11]. At normal emission, corresponding to the  $\Gamma$  point in the Brillouin

zone (BZ), the spectrum exhibits a main peak at 1 eV, followed by a linear slope between 0.6 eV and  $E_F$ . As expected, this band feature does not disperse in a direction perpendicular to the chains. However, we did not observe any dispersion even along the chain direction but only slight intensity variations. In particular, we could not determine any Fermi surface crossing. These features are common to all the Bechgaard salts we have investigated, of both the (TMTSF) and (TMTTF) families, and indicate the absence of dispersing quasiparticle peaks (Fig. 1c).

The only material-dependent changes are small rigid shifts of the spectral leading edges in the (TMTTF) salts. The high-resolution normal emission data of Figure 3b are representative of the results obtained throughout the BZ. A linear fit of the leading edge defines a crossing of the baseline near  $E_F$  in (TMTSF)<sub>2</sub>PF<sub>6</sub> (and ClO<sub>4</sub>). On the other hand, the baseline crossing is at  $\Delta \sim 100$  meV for (TMTTF)<sub>2</sub>PF<sub>6</sub>, and  $\Delta \sim 30$  meV for (TMTTF)<sub>2</sub>Br. Since all spectra are referred to a common Fermi level, the shifts indicate energy gaps ( $E_{\text{gap}} \sim 2\Delta$ ) in the (TMTTF) salts. The smaller shift for (TMTTF)<sub>2</sub>Br is consistent with its narrower gap. This interpretation is supported by recent data on (TMTSF)<sub>2</sub>ReO<sub>4</sub>. The spectra of that material exhibit a transition from a “pseudogap-like” lineshape to a real gap, in correspondence of the anion ordering metal-insulator transition at 180 K (not shown) [4,30].

The null value for the TMTSF compounds is compatible with their metallic behavior but, taking into account the thermal and experimental broadening, we cannot definitely exclude a small (up to  $\sim 10$  meV) gap. The spectra of Figure 3 unambiguously establish the insulating character of the TMTTF samples. However, ARPES only probes the occupied states, and some care is necessary when the measured shifts are used to estimate the gap values. For instance, if the Fermi level was pinned by impurities at the bottom of the conduction band, our analysis would overestimate the gap by a factor 2. On the other hand, it is likely that pinning defects will act in a similar way for all the members of the (TMTTF) family, so that all gaps will be similarly over- or underestimated.

### 2.3 Optics

By combining the results from different spectrometers in the microwave, millimeter, submillimeter, infrared, visible and ultraviolet ranges, we have obtained the electrodynamic response of these Bechgaard salts over an extremely broad range ( $10^{-5}$ –10 eV) [6,7]. At all frequencies up to and including the midinfrared, we placed the samples in an optical cryostat and measured the reflectivity as a function of temperature between 5 and 300 K [6,7]. In the optical range from  $2 \times 10^{-3}$  to 10 eV, the polarized reflectance measurements were performed, employing four spectrometers with overlapping frequency ranges; while in the microwave and millimeter wave spectral range, the spectra were obtained by the use of a resonant cavity perturbation technique [6,7,12].

Figure 4 summarizes the temperature dependence of the real part  $\sigma_1(\omega)$  of the optical conductivity in different

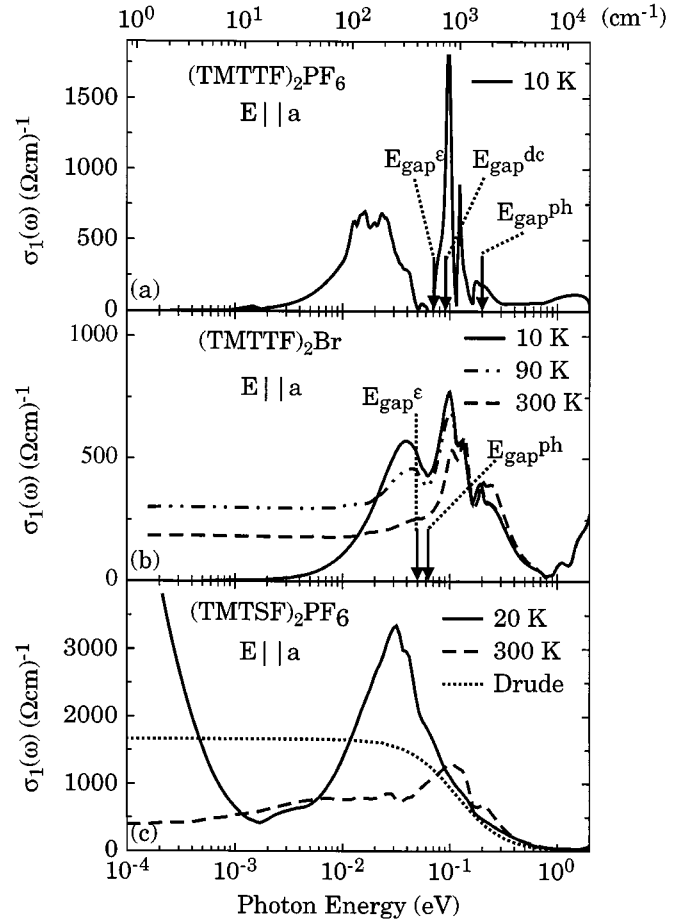


**Fig. 4.** On chain optical conductivity of (a) (TMTTF)<sub>2</sub>PF<sub>6</sub>, (b) (TMTTF)<sub>2</sub>Br, and (c) (TMTSF)<sub>2</sub>PF<sub>6</sub> at temperatures above the transitions to the broken symmetry states. The arrows indicate the gaps observed by dielectric ( $\epsilon$ ) response, dc resistivity and photoemission (ph). A simple Drude component is also shown in part (c). Note that photoemission measures the quantity  $E_{\text{gap}}/2$ , assuming that the Fermi level is in the middle of the gap.

Bechgaard salts for  $E||a$ , the chains direction. Part (a) and (b) show  $\sigma_1(\omega)$  for the PF<sub>6</sub> and Br compounds of the TMTTF family, while part (c) displays  $\sigma_1(\omega)$  for (TMTSF)<sub>2</sub>PF<sub>6</sub>. We can immediately remark that the temperature dependence of  $\sigma_1(\omega)$  is quite important in all compounds, except in (TMTTF)<sub>2</sub>PF<sub>6</sub>, which is basically in an insulating state at all temperatures. The data presented here are in broad agreement with previous, less detailed studies [5,31], and they include frequencies below the conventional optical spectra.

The optical conductivity of the TMTTF salts displays several transitions with large absorption features due to lattice vibrations (phonon modes), mainly due to the inter and intramolecular vibrations of the TMTTF (and TMTSF) unit. These vibrations can be even enhanced by the electron-phonon coupling [31]. The phonon modes are particularly observed in the TMTTF salts, because the screening by free electrons is less effective. Although it is clear that the optical properties of the TMTTF salts are

those of a semiconductor, with a gap for the charge excitations, the evaluation of the magnitude of the gap, based on the optical spectra, is not straightforward, because of the large phonon activity. Thus, the results of other measurements were used to evaluate the gap. The dc conductivity as well as the low-temperature dielectric constant ( $\epsilon$ ) measured at 100 GHz are consistent with  $E_{\text{gap}} = 87$  and 50 meV for (TMTTF)<sub>2</sub>PF<sub>6</sub> and (TMTTF)<sub>2</sub>Br, respectively [12,32]. These results also suggest that the absorption in  $\sigma_1(\omega)$  near 99 meV for (TMTTF)<sub>2</sub>PF<sub>6</sub> is associated with  $E_{\text{gap}}$ ; this is supported by the fact that this feature has the correct spectral weight [12]. Moreover, for the (TMTTF)<sub>2</sub>Br below 90 K (*i.e.*, at  $T < T_p$ ) there is the progressive disappearance of the spectral weight, defined as  $\int_0^{\omega_c} d\omega \sigma_1(\omega)$  with  $\omega_c$  a cut-off frequency, in FIR (*i.e.*,  $\omega < 37$  meV) with decreasing temperatures. The missing spectral weight mainly piles up at the gap feature around 50 meV. The photoemission experiments suggest a gap of 0.2 eV for (TMTTF)<sub>2</sub>PF<sub>6</sub> and 60 meV for (TMTTF)<sub>2</sub>Br (see Fig. 3 and the discussion in Sect. 2a). The gap values obtained for (TMTTF)<sub>2</sub>X with different techniques are displayed in Figure 4. Because the band is partially filled, the charge gap in both of the (TMTTF)<sub>2</sub>X salts is a correlation rather than a single-particle gap.

The optical properties of the (TMTSF)<sub>2</sub>X analogs, for which the dc conductivity gives evidence for metallic behaviour down to low temperatures (to the transition to the spin density wave state at  $T_{\text{SDW}}$ ), are markedly different from those of a simple metal. A well-defined gap feature around 25 meV and a zero-frequency mode [6,7,12,33] are observed at low temperatures. The latter mode at low temperatures is narrower in (TMTSF)<sub>2</sub>ClO<sub>4</sub> (not shown here) than in (TMTSF)<sub>2</sub>PF<sub>6</sub> [12]. The combined spectral weight of the two modes is in full agreement with the known carrier concentration of  $1.4 \times 10^{21} \text{ cm}^{-3}$  and a band mass that is very close to the electron mass [4]. For both (TMTSF)<sub>2</sub>X salts, the zero-frequency mode has small spectral weight on the order of 1% of the total. Nevertheless, this mode is responsible for the large metallic conductivity. Figure 4c also indicates that the two components of  $\sigma_1(\omega)$  clearly develop at low temperatures. In fact, there is a progressive narrowing of the effective metallic contribution to  $\sigma_1(\omega)$  with decreasing temperatures. Moreover, the dc-limit of  $\sigma_1(\omega)$  is in fair agreement with  $\sigma_{\text{dc}}$  values from the transport data, as also confirmed by the so-called Hagen-Rubens extrapolation of our original absorption or reflectivity measurements [12,34].

### 3 Discussion

Both photoemission and optical data indicate that the spectral properties of the metallic Bechgaard salts are incompatible with those of a simple metal (Figs. 1b, c). The photoemission spectra reveal a strong suppression of spectral weight near the chemical potential and the absence of dispersing quasiparticle features. The optical response

is complex, and cannot be described by a simple Drude component.

A standard interpretation of the angle-integrated spectrum of (TMTSF)<sub>2</sub>PF<sub>6</sub> would suggest a deep pseudogap, with a vanishingly small DOS at the Fermi level. This, however, is incompatible with transport data (Fig. 2), and with optics, which shows no evidence for such a broad ( $\sim 0.5$  eV) pseudogap (Fig. 4 and discussion below). The 1D properties of (TMTSF)<sub>2</sub>PF<sub>6</sub> suggest to interpret the spectrum as the incoherent power-law background  $\rho(\omega) = |\omega|^\alpha$  of the Luttinger model (Figs. 1a, c). The exponent  $\alpha$  reflects the strength of the interactions, and is related to the fundamental charge correlation parameter  $K_\rho$  of the Luttinger model by the expression  $\alpha = (K_\rho + K_\rho^{-1} - 2)/4$ . An analysis of the experimental data yields  $K_\rho \sim 0.2$ , with rather large error bars due to the finite temperature, and the uncertainties over the energy range where the asymptotic Luttinger expression applies [24]. Anyway,  $K_\rho$  is well below the 1/2 limit of the standard Hubbard model. This indicates strong and long-range electronic correlations, in qualitative agreement with optics, and with the conclusions of NMR and transport investigations [17,20,35,36].

The ARPES data should be compared with the  $k$ -dependent spectral function  $A(k, \omega)$  of the Luttinger model [8,9]. The spectra of Figure 3 certainly do not exhibit the characteristic spinon and holon peaks. However, Voit [2] has shown that the appearance of the TLL spectral function is drastically modified for large values of the exponent  $\alpha$ , which may be relevant here. In this parameter range the holon peak is reduced to a cusp singularity, and the spinon is replaced by a ( $k$ -dependent) low energy tail. These aspects of a large- $\alpha$  TLL are qualitatively consistent with the experimental lineshapes.

The Luther-Emery model provides a more appropriate scenario for the insulating (TMTTF) salts. For moderately strong interactions (small  $\alpha$  values) the LE spectral function exhibits separate spin and charge features, although the intensity distribution is not identical to that of the TLL spectral function [2]. We may speculate that, with increasingly strong correlations, and larger  $\alpha$ , the evolution of the LE and TLL lineshape will be similar, *i.e.* towards a strong suppression of intensity near  $E_F$ .

A Luttinger (or Luther-Emery)-like interpretation faces two main objections: the unexpectedly large value of  $\alpha$ , and the absence of any  $k$ -dependence in the ARPES spectra.  $\alpha$  values of the order of 1 are incompatible with results for the standard Hubbard model; for purely local interactions, in fact,  $K_\rho > 1/2$  ( $\alpha < 1/8$ ). Smaller  $K_\rho$  (larger  $\alpha$ ) values are possible for longer-range interactions. Lower limits are then set by Umklapp scattering, which becomes relevant at commensurate filling. Exactly at quarter-filling the system is insulating for  $K_\rho < 1/4$  ( $\alpha > 9/16$ ). This is indeed the parameter range suggested by optics (see below). Slightly away from 1/4 filling, a doped 1D chain can still exhibit TLL behavior with  $K_\rho$  as small as 1/8, and  $\alpha$  as large as 1.53 [37], within the correlation gap, on the energy scale of the dopant band. However, this energy scale is more than one order of magnitude smaller than the energy range (the pseudogap) over

which the photoemission spectra exhibit non-Fermi liquid behavior. Moreover, at such low energies, the physics of a real system is likely to be anyway dominated by transverse interactions.

The lack of dispersion in the ARPES spectra is equally puzzling. Even for a large- $\alpha$  TLL, where the spectral peaks are considerably smeared, theory [2,9] predicts that the leading edge of the spectral function should exhibit a  $k$ -dependence. In this respect, it is interesting to compare the present results with the data on the 1D organic conductor TTF-TCNQ [38]. Also in that case the ARPES spectra suggest non-Fermi liquid behavior, and an exponent close to 1, but the (anomalous) spectral features disperse with the periodicity of the lattice. Dispersing features have also been reported for the (half-filled) 1D Mott insulators SrCuO<sub>2</sub> and Sr<sub>2</sub>CuO<sub>3</sub> [39,40].

The absence of dispersion suggest that, within the probing depth of photoemission, the electronic states of the Bechgaard salts are localized. Localization could be due to surface-specific defects like cleavage steps, or a modified surface stoichiometry, which do not affect the bulk of the sample. The peculiar lineshapes of the angle-integrated and angle-resolved spectra, and the absence of dispersion, could be considered as an indirect manifestation of the TLL phenomenology (*via* the extreme sensitivity to defect-induced localization) and strong 1D correlations. Interestingly, in a TLL with impurities, the values of  $K_\rho$  are not modified, but the usual critical exponents are replaced by new, renormalized “boundary exponents” [41,42]. In a 1/4 filled system, the critical  $K_\rho = 1/4$  for a Mott transition would yield  $\alpha = 1.5$ . Therefore, in the presence of impurities, exponents as large as 1.5 may be compatible with a small charge gap. If such large  $\alpha$  values are actually realized, we can expect them to smear any subtle differences between the various Bechgaard salts, and thus yield the observed material-independent lineshape. Of course, the relative rigid shift reflecting overall variations of the chemical potential, would still survive.

Focusing now our attention on the optical response (Fig. 4), we note that it is mainly characterized by the gap-like feature in all compounds and by the narrow zero frequency mode in the (TMTSF) salts only. In both cases, due to full charge transfer from the organic molecule to the counter ions, the TMTTF or TMTSF stacks have a quarter-filled hole band. There is also a moderate dimerization, which is somewhat more significant for the TMTTF family [4]. Therefore, depending on the importance of this dimerization, the band can be described as either half-filled (for a strong dimerization effect) or quarter-filled (for weak dimerization). Due to the commensurate filling, a strictly one-dimensional (Luttinger) model is expected to lead to a Mott insulating behaviour (Fig. 1b). Indeed, the (TMTTF)<sub>2</sub>X salts, with X = PF<sub>6</sub> or Br, are insulators at low temperatures [4] with a substantial (Mott) charge gap (see Figs. 3 and 4). For these compounds the correlation gap is so large that the interchain hopping (defined by  $t_b$ ) is suppressed by the insulating nature of the 1D phase and is not relevant.

It thus seems very natural to interpret the high frequency part of the optical conductivity in terms of a Mott insulator (Fig. 1b). Due to the apparent contradiction of having a rather large (Mott) correlation gap ( $\sim 12$  meV) and a good metallic dc conductivity in the (TMTSF) family, it was proposed that the peak structure was due to the dimerization gap  $\Delta_{\text{dim}}$  [31,43]. This would indeed be the case for an extremely strong (nearly infinite) repulsion, with the quarter-filled band being transformed into a half-filled band of (nearly noninteracting) spinless fermions. It was then argued that the real charge gap of the problem was smaller, on the order of 50 K.

However, such an interpretation fails to reproduce the observed frequency dependence above the peak in conductivity. At frequencies greater than  $t_b$ , the interchain electron transfer is irrelevant and calculations based on the 1D Hubbard model should be appropriate. Such calculations result in a frequency-dependent conductivity  $\sigma_1(\omega) \sim \omega^{-\gamma}$  (where  $\gamma = 4n^2K_\rho - 5$ ) for frequencies greater than  $t_b$  and  $E_{\text{gap}}$  but less than the on-chain bandwidth  $4t_a$  (Fig. 1b) [3]. Our results can be described with an exponent  $\gamma = 1.3$  for both (TMTSF)<sub>2</sub>X compounds [7,12]. Using the same type of analysis for the conductivity as in reference [37], and attributing the peak to the dimerization gap, results in  $\sigma_1(\omega) \sim 1/\omega^3$  for  $\omega \gg \Delta$ , as in a simple semiconductor (corresponding to nearly free spinless fermions). The observed power law (see Fig. 4 in Ref. [12]) differs significantly from this prediction, making such an interpretation of the data very unlikely. The exponent  $\gamma$  can in principle be used to obtain the Luttinger liquid parameter  $K_\rho$ , which controls the decay of all correlation functions [3,7]. From our value for  $\gamma$  and the assumption that quarter-filled band Umklapp scattering (*i.e.*, with  $n = 2$  then  $\gamma = 16K_\rho - 5$ ) is dominant in the TMTSF family, we obtain  $K_\rho \sim 0.23$  [7], which is in reasonable agreement with photoemission (Fig. 3) [10,11] and transport data [17,20].

We now turn to the issue about the apparent contradiction between a good metallic dc conductivity and a large Mott gap in the (TMTSF) family. As anticipated above, such a situation is realized when the system is doped slightly away from commensurate filling (Fig. 1b) [3]. Indeed, this is what seems to be observed here (Fig. 4), with the “Drude” peak in the TMTSF family containing only 1% of the carriers (*i.e.*, 1% of the total spectral weight obtained by integrating  $\sigma_1(\omega)$  up to  $\omega_c \sim 1$  eV). Although no real doping exists from a chemistry point of view, one could attribute such a deviation from commensurability to the effects of interchain hopping. If single-particle hopping ( $t_b$ ) between chains is relevant, small deviations from commensurate filling due to the warping of the Fermi surface exist, and should lead to effects equivalent to real doping on a single chain. Of course, such a picture is only a poor man’s way of viewing the low-frequency structure. Since the interchain hopping is relevant, the low-frequency peak should in principle be described by a full two-dimensional theory of interacting fermions [3].

The dimensionality crossover, induced by the increasing  $t_b$  upon pressure or by changing the chemistry from

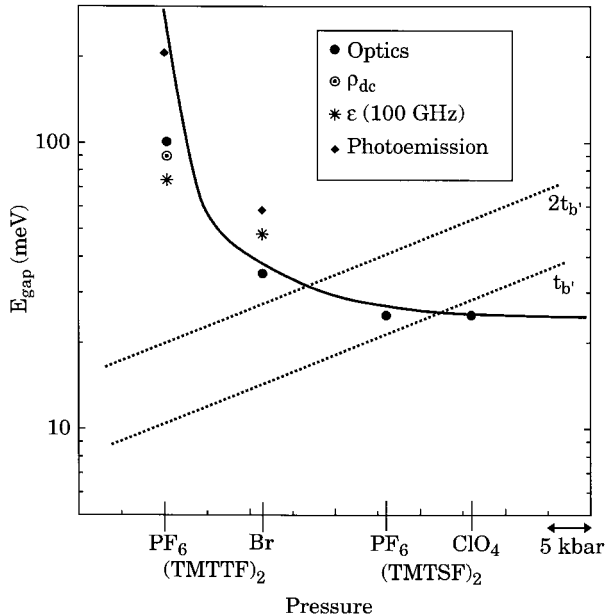


**Fig. 5.** The pressure dependence of the (Mott) correlation gap, as established by different experimental methods, and of the transfer integral, perpendicular to the chains,  $t_b$ , for the Bechgaard salts. The horizontal scale was derived with the results of pressure studies [4,20].

the TMTTF to the TMTSF family, is one of the central issues. There is a well-established order for  $t_b$  among the four salts investigated. The  $(\text{TMTTF})_2\text{X}$  analogs are more anisotropic, and the transfer integrals are approximately given by  $t_a:t_b:t_c = 250:10:1$  meV [4]. For the  $(\text{TMTSF})_2\text{X}$  analogs, the transfer integrals are about 250:25:1 meV. The values for both groups of salts are in broad agreement with tight-binding model calculations and with the trend indicated by the plasma frequency [7, 12, 44]. To arrive at a scale for  $t_b$ , we took the calculated values as averages for the  $(\text{TMTSF})_2\text{X}$  and  $(\text{TMTTF})_2\text{X}$  salts, respectively, and assumed that pressure changes  $t_b$  in a linear fashion. The positions of the various salts along the horizontal axis of Figure 5 reflect this choice [12], with pressure values taken from the literature; such a scale has been widely used when discussing the broken symmetry ground states of these materials [4].

The solid line in Figure 5 represents the overall behaviour of the correlation gap (see also Figs. 3 and 4). Various experiments give slightly different values of the gap. This is probably due to the differences in the curvature of the band which is scanned differently by different experiments, or due to the different spectral response functions involved. The decrease going from the  $(\text{TMTTF})_2\text{X}$  to the  $(\text{TMTSF})_2\text{X}$  analogs may represent various factors [45], such as the decreasing degree of dimerization and the slight increase in the bandwidth along the chain direction, as evidenced by the greater value of the plasma frequency measured along the chain direction in the  $(\text{TMTSF})_2\text{X}$  salts [12,31]. The dotted line representing  $2t_b$  (this is half the bandwidth perpendicular to the chains in the tight-binding approximation) crosses the full

line displaying the behaviour of  $E_{\text{gap}}$  between the salts exhibiting insulating and metallic behaviour, whereas the dotted line representing  $t_b$  crosses the solid line between the two metallic salts. Therefore, our experiments strongly suggest that a crossover from a non-conducting to a conducting state occurs when the unrenormalized single particle transfer integral between the chains exceeds the correlation gap by a factor  $A$ , which is on the order of but somewhat greater than 1.

Additional evidence for a pronounced qualitative difference between states with  $At_b < E_{\text{gap}}$  and  $At_b > E_{\text{gap}}$  is given by plasma frequency studies along the  $b'$  direction (*i.e.*, perpendicular to the chain). As shown in reference [12], there is no well-defined plasma frequency for the insulating state, and we regard this as evidence for the confinement [46] of electrons on individual chains. In fact, the reflectivity has a temperature independent overdamped like behaviour. Conversely, the electrons become deconfined as soon as  $At_b \sim E_{\text{gap}}$  (Fig. 5). Such a deconfinement is manifested by the onset of a sharp plasma edge in the low-temperature reflectivity spectra of the  $(\text{TMTSF})_2\text{X}$  salts along the  $b'$  axis [12]. This conclusion is not entirely unexpected: a simple argument (the same as one would advance for a band-crossing transition for an uncorrelated band semiconductor) would suggest that to create an electron hole pair with the electron and hole residing on neighbouring chains, an energy comparable to the gap would be required.

Various theories [46–50] suggest a strong renormalization of the relevant interchain transfer integral  $t_b^{\text{eff}} = t_b(t_b/t_a)^{(\alpha/1-\alpha)}$  [48], substantially smaller than  $t_b$ , for coupled Luttinger liquids. Some of these studies [46–49], however, do not take into account the periodicity of the underlying lattice and the resulting Umklapp scattering. Such a scattering has a marked influence on the effect of interchain transfer. A renormalization group treatment [49] of two coupled Hubbard chains predicts a crossover between confinement (that is, no interchain single-electron charge transfer) and deconfinement, at  $At_b^{\text{eff}} = E_{\text{gap}}$ , with the value of  $A$  estimated to be between 1.8 and 2.3. A transition or crossover from an insulator to a metal has also been conjectured by Bourbonnais [50], on the basis of studies of arrays of coupled chains, where also Umklapp scattering has been taken into account. We notice that, for the large  $\alpha$  exponents discussed previously, the above formula would yield unreasonably low values of  $t_b^{\text{eff}}$ . Such small values are both incompatible with  $t_b^{\text{eff}} = E_{\text{gap}}/A \sim 10\text{--}20$  meV estimated from experiment, and with the observed metallic behaviour in the TMTSF salts at low frequency [7].

Discrepancies between theoretical predictions and experimental estimates are not totally surprising, if one considers that the experiment probes the transverse optical response over an energy scale of about 0.1 eV. At these energies, self-energy effects at the origin of the renormalization of  $t_b$  may be irrelevant. It follows that from optics,  $t_b^{\text{eff}}$  can be closer to the bare  $t_b$ . In that sense, the onset of the transverse plasma edge as a function of (chemical)

pressure may not coincide with the one found from low-energy probes like dc transport [20] and NMR [35].

We also note that, in the absence of pressure-dependent optical studies, it remains to be determined whether the onset of the transverse plasma edge [12] which we observe going from the  $(\text{TMTTF})_2\text{X}$  to  $(\text{TMTSF})_2\text{X}$  salts, coincides with the insulator-to-metal transition found in transport [20] and nuclear magnetic resonance (NMR) measurements [35]. Although optical experiments under pressure are difficult to conduct, studies of the pressure dependence of the dielectric constant, combined with dc transport data, could clarify this issue.

The existence of a gap feature in the metallic state, containing nearly all of the spectral weight, is at first sight similar to what is expected for a band-crossing transition for simple semiconductors, which would result in a semimetallic state. However, the nearly temperature-independent magnetic susceptibility [4], which gives strong evidence for a gapless spin excitation spectrum (this has often been interpreted as a Pauli susceptibility or as the susceptibility due to a large exchange interaction), demonstrates that the state is not a simple semimetal. The existence of a gap, or pseudogap in the charge excitations (Figs. 3 and 4) with the absence of a gap for spin excitations, indicates charge-spin separation in the metallic state. This charge-spin separation is, however, distinct from that of a 1D TLL, in which both excitations are gapless but have different velocities. Here, it is the Umklapp scattering which leads to gapped charge excitations. The nature of the metallic state may be close to that of a doped 1D Mott-Hubbard semiconductor [3, 51], where the inter-chain transfer results in deviations from half- (or quarter-) filling on each chain and therefore has an effect similar to (self-) doping [3, 7, 17, 52].

## 4 Conclusion

Both photoemission and optical data reveal the peculiarity of the one-dimensional interacting electron gas response. The unusual spectral features of the Bechgaard salts prove that these materials are certainly not simple anisotropic band metals. Clear deviations from the Fermi liquid behaviour have been identified and several aspects hint to a possible manifestation of a Tomonaga-Luttinger or Luther-Emery liquid in the normal phases [16, 17]. Interestingly, optics and photoemission reveal such deviations on different energy scales. The characteristic energy scale in the optical conductivity data is the Mott-Hubbard gap, of about  $\sim 12$  meV in  $(\text{TMTSF})_2\text{PF}_6$ . The salient feature of the photoemission spectra is the much larger ( $\sim 10^2$  meV) pseudogap. Both techniques, on the other hand, point to a characteristic Luttinger parameter  $K_\rho \sim 0.2$ , and therefore to strong, long-range 1D correlations. Also, both the photoemission and optics data discriminate between the conducting (TMTSF) and the insulating (TMTTF) salts, with a reasonable agreement on the gap size of the latter.

Several issues concerning the electronic structure of these materials are still open, and it is not yet clear

whether a comprehensive description is possible within the existing theoretical scenarios. The optical response in the TMTSF salts has been interpreted in terms of a dimensionality crossover induced by the interchain coupling. Nevertheless, an incipient 2D Fermi liquid behaviour at low temperature and frequency [17, 20] is *de facto* described starting from the 1D TLL theory, instead of a two-dimensional approach. Even in a 1D framework, there is no clear justification for using the results of the Luttinger model in the presence of a charge gap. It may be argued that, for small gaps, the typical correlations of the TLL liquid will still manifest themselves at frequencies (energies) larger than the gap. However, theoretical work is certainly necessary to put these speculations on firmer ground. Also, it remains to be explained why theory predicts the confinement-deconfinement crossover when  $E_{\text{gap}}$  is of the order of the renormalized transfer integral  $t_b^{\text{eff}}$ , while experimentally the bare  $t_b$  seems to be relevant. It seems that a theory of the dimensionality crossover in coupled Luttinger liquid that would be completely consistent with the present data is still lacking. In fact, it is a common theoretical opinion that a large  $\alpha$  exponent should prevent any coherent transport, even though the Mott gap can be overcome by a large  $t_b$ . As far as photoemission is concerned, the absence of dispersion, which is not a general feature of quasi-1D systems, is puzzling. The ARPES experimental results point towards localized states and renormalized exponents near the surface. There are indications that these surface effects are related to the 1D nature of the materials, but no clear theoretical picture is yet available. Such specific details may eventually prevent the development of a comprehensive framework for the spectral properties of the Bechgaard salts. Further investigations of the effects of disorder, and of possible anomalous effects in the photoexcitation process in 1D, not considered in a standard approach, could contribute to clarify these discrepancies.

The authors are very grateful to C. Bourbonnais, P.M. Chaikin, M. Dressel, T. Giamarchi, D. Jérôme, F. Mila and J. Voit for many illuminating discussions. Research at ETH Zurich and EPF Lausanne was supported by the Swiss National Science Foundation. Research at UCLA by NSF grant DMR-9503009 and at Indiana University by NSF grant DMR-9414268, and at SRC by NSF grant DMR-95-31009.

## References

1. J. Luttinger, *J. Math. Phys.* **4**, 1154 (1963); S. Tomonaga, *Prog. Theor. Phys.* **5**, 554 (1950); for a review, see H.J. Schulz, *Int. J. Mod. Phys. B* **5**, 57 (1991).
2. J. Voit, *Eur. Phys. J. B* **5**, 505 (1998); in *Proceedings of the NATO Advanced Research Workshop on The Physics and Mathematical Physics of the Hubbard Model, San Sebastian, October 3-8, 1993*, edited by D. Baeriswyl, D.K. Campbell, J.M.P. Carmelo, F. Guinea, E. Louis (Plenum Press, New York, 1995).
3. T. Giamarchi, *Physica B* **230-232**, 975 (1997).
4. D. Jérôme, H.J. Schulz, *Adv. Phys.* **31**, 299 (1982).



5. C.S. Jacobsen *et al.*, Phys. Rev. Lett. **46**, 1142 (1981); Solid State Commun. **38**, 423 (1981); Phys. Rev. B **28**, 7019 (1983).
6. M. Dressel *et al.*, Phys. Rev. Lett. **77**, 398 (1996).
7. A. Schwartz *et al.*, Phys. Rev. B **58**, 1261 (1998).
8. V. Meden, K. Schönhammer, Phys. Rev. B **46**, 15753 (1992).
9. J. Voit, J. Phys. Cond. Matter **5**, 8305 (1993).
10. B. Dardel *et al.*, Europhys. Lett. **24**, 687 (1993).
11. F. Zwick *et al.*, Phys. Rev. Lett. **79**, 3982 (1997).
12. V. Vescoli *et al.*, Science **281**, 1181 (1998).
13. K. Bechgaard *et al.*, Solid State Commun. **33**, 1119 (1980).
14. G. Grüner, Rev. Mod. Phys. **60**, 1129 (1988).
15. G. Grüner, in *Density Waves in Solids* (Addison-Wesley, Reading, MA, 1994).
16. D.G. Clarke *et al.*, Science **279**, 2071 (1988).
17. C. Bourbonnais, D. Jérôme, cond-mat/9903101.
18. V.J. Emery *et al.*, Phys. Rev. Lett. **48**, 1039 (1982).
19. The  $b'$  and  $c'$  directions are perpendicular to the chain direction  $a$ . These directions also define the faces of the samples on which the optical experiments were conducted and are slightly different from the  $b$  and  $c$  directions of the unit cell because of the triclinic crystal structure. This small difference does not influence the arguments advanced in this work.
20. J. Moser *et al.*, Eur. Phys. J. B **1**, 39 (1998).
21. C. Coulon *et al.*, J. Phys. France **43**, 1059 (1982).
22. J.P. Pouget *et al.*, Mol. Cryst. Liq. Cryst. **79**, 129 (1982).
23. P.M. Grant, J. Phys. Colloq. France **44**, C3-847 (1983).
24. B. Dardel *et al.*, Phys. Rev. Lett. **67**, 3144 (1991).
25. A. Sekiyama *et al.*, Phys. Rev. B **51**, 13899 (1995).
26. T. Takahashi, Phys. Rev. B **53**, 1790 (1996).
27. Y. Hwu *et al.*, Phys. Rev. B **46**, 13624 (1992).
28. G.-H. Gweon *et al.*, J. Phys. Cond. Matter **8**, 9923 (1993).
29. M. Grioni *et al.*, Phys. Scr. T **66**, 172 (1996).
30. F. Zwick *et al.*, Solid State Commun. **113**, 179 (2000).
31. D. Pedron *et al.*, Phys. Rev. B **49**, 10893 (1994).
32. S.E. Brown (private communication).
33. N. Cao, T. Timusk, K. Bechgaard, J. Phys. I France **6**, 1719 (1996).
34. W. Henderson *et al.*, Eur. Phys. J. B **11**, 365 (1999).
35. P. Wzietek *et al.*, J. Phys. I France **3**, 171 (1993).
36. C. Bourbonnais *et al.*, J. Phys. Lett. France **45**, L-755 (1984).
37. T. Giamarchi, Phys. Rev. B **44**, 2905 (1991).
38. F. Zwick *et al.*, Phys. Rev. Lett. **81**, 2974 (1998).
39. C. Kim *et al.*, Phys. Rev. Lett. **77**, 4054 (1996).
40. H. Fujisawa *et al.*, Solid State Commun. **106**, 543 (1998).
41. S. Eggert, H. Johanneson, A. Mattson, Phys. Rev. Lett. **76**, 1505 (1996).
42. Y. Wang, J. Voit, F.-C. Pu, Phys. Rev. B **54**, 8491 (1996).
43. F. Favand, F. Mila, Phys. Rev. B **54**, 10435 (1996).
44. L. Ducasse *et al.*, J. Phys. C **19**, 3805 (1986).
45. K. Penc, F. Mila, Phys. Rev. B **50**, 11429 (1996).
46. P.W. Anderson, Proc. Natl. Acad. Sci. U.S.A. **92**, 6668 (1995).
47. F. Mila, D. Poilblanc, Phys. Rev. Lett. **76**, 287 (1996).
48. C. Bourbonnais, L.G. Caron, Int. J. Mod. Phys. B **5**, 1033 (1998).
49. Y. Suzumura *et al.*, Phys. Rev. B **57**, R15040 (1991).
50. C. Bourbonnais, in *Strongly interacting fermions and high  $T_c$  superconductivity*, edited by B. Doucot, J. Zinn-Justin (Elsevier, Amsterdam, 1995), p. 307.
51. H. Mori *et al.*, J. Phys. Soc. Jap. **63**, 1639 (1994).
52. N. Bulut *et al.*, Phys. Rev. Lett. **72**, 705 (1994).